Author(s): Artault, Maxime; Gonzalez, Gabriel; Damlin, Pia; Toivola, Juho; Mailman, Aaron; Hannonen, Jenna; Pihko, Petri M.; Peljo, Pekka

Title: Azoniafluorenones : A New Family of Two-Electron Storage Electrolytes for Sustainable Near-Neutral pH Aqueous Organic Flow Battery

Year: 2024

Version: Published version

Please cite the original version:

Artault, M., Gonzalez, G., Damlin, P., Toivola, J., Mailman, A., Hannonen, J., Pihko, P. M., & Peljo, P. (2024). Azoniafluorenones : A New Family of Two-Electron Storage Electrolytes for Sustainable Near-Neutral pH Aqueous Organic Flow Battery. Advanced Energy Materials, Early online. https://doi.org/10.1002/aenm.202401635

ADVANCED ENERGY MATERIALS
www.advenergymat.de

Azoniafluorenones: A New Family of Two-Electron Storage Electrolytes for Sustainable Near-Neutral pH Aqueous Organic Flow Battery

Maxime Artault, Gabriel Gonzalez, Pia Damlin, Juho Toivola, Aaron Mailman, Jenna Hannonen, Petri M Pihko, and Pekka Peljo**

Fluorenones are suitable candidates for negolytes in flow batteries, as they demonstrate the ability to store 2 electrons, and can achieve reversibility, solubility, and stability with appropriate molecular design. However, limitations persist such as the use of alkaline media, high redox potentials, and a limited scope for optimization. Herein, azoniafluorenones is reported as a novel class of negolytes. They can be readily accessed in a highly modular fashion from inexpensive commercially available materials (e.g., boronic acids). Variations in the substitution patterns reveal the 3-substituted *N*-alkylated AZON3, which demonstrates excellent solubility at neutral pH (1.64 M) with two low reversible redox potentials (−0.31 and −0.58 V vs Ag/AgCl). AZON3 exhibits high stability when evaluated at high concentration in a neutral supporting electrolyte (1 M in 3 M KCl), paired with BTMAP-Fc on the positive side. Capacity retentions of 99.95% and 99.91% per cycle (99.35% and 99.21% per day) are achieved when cycling with 1 and 2 electrons, respectively, coupled with high volumetric capacity of 46.4 Ah L^{-1} (87% of capacity utilization).

1. Introduction

There is an urgent need to develop affordable, scalable, and secure energy storage to enable the integration of a growing amount of renewable energy sources like wind and solar power into the electrical grids.[1] Flow batteries (FBs) offer a possible solution to this challenge due to their safety features, cost-effectiveness, long-term durability, and the ability to adjust energy/power levels.[2,3] In a FB, the active ingredients are circulated through the cell stack from tanks, preferably as aqueous solutions.[4,5] The first generation of aqueous FBs use transition metal-based electrolytes, with vanadium flow batteries (VFBs) being close to commercialization. However, the high cost and toxicity concerns of vanadium remain an obstacle to the widespread adoption of VFBs.[6]

Aqueous organic flow batteries (AOFBs)[7,8] can be operated in alkaline and acidic solutions, but operation at near-neutral pH would significantly reduce the operational risks and corrosion of the tank and pump materials.[9,10] A corrosive environment requires more robust and durable materials while a neutral environment could allow inexpensive and easily manufacturable components and ultimately reduce costs for supporting the large-scale commercialization of AOFBs.

One limitation of AOFBs is their energy density, which is dependent on the solubility of the organic compound dissolved in the aqueous electrolyte. However, the energy density can also be improved by increasing the number of electrons that the redox species can transfer/store. Despite progress in this topic,[11,12] there is a need for additional approaches that focus on developing negolytes with low redox potential, capable of storing more than one electron while maintaining good stability during long-term cycling.

Examples of compounds demonstrating a reversible two-electron redox cycle include phenazines,[13,14] viologens,[15,16] anthraquinones,[17,18] and fluorenone[19–21] derivatives. Recently, a novel pyridinium-functionalized fluorenone compound, known as (OTDFL)Cl_2,[21] was developed based on the fluorenone 4C7SFL (see **Figure 1a**).[20] (OTDFL)Cl_2 has excellent solubility in water and it can store two electrons under neutral

M. Artault, J. Toivola, A. Mailman, P. M Pihko
Department of Chemistry and NanoScience Centre
University of Jyväskylä
JYU
P.O.B. 35, Jyväskylä FI-40014, Finland
E-mail: petri.pihko@jyu.fi

G. Gonzalez, J. Hannonen, P. Peljo
Research Group of Battery Materials and Technologies
Department of Mechanical and Materials Engineering
University of Turku
Vesilinnantie 5, Turku FI-20014, Finland
E-mail: pekka.peljo@utu.fi

P. Damlin
Materials Chemistry Research Group
Department of Chemistry
University of Turku
Henrikinkatu 2, Turku FI-20500, Finland

The ORCID identification number(s) for the author(s) of this article can be found under https://doi.org/10.1002/aenm.202401635

DOI: 10.1002/aenm.202401635

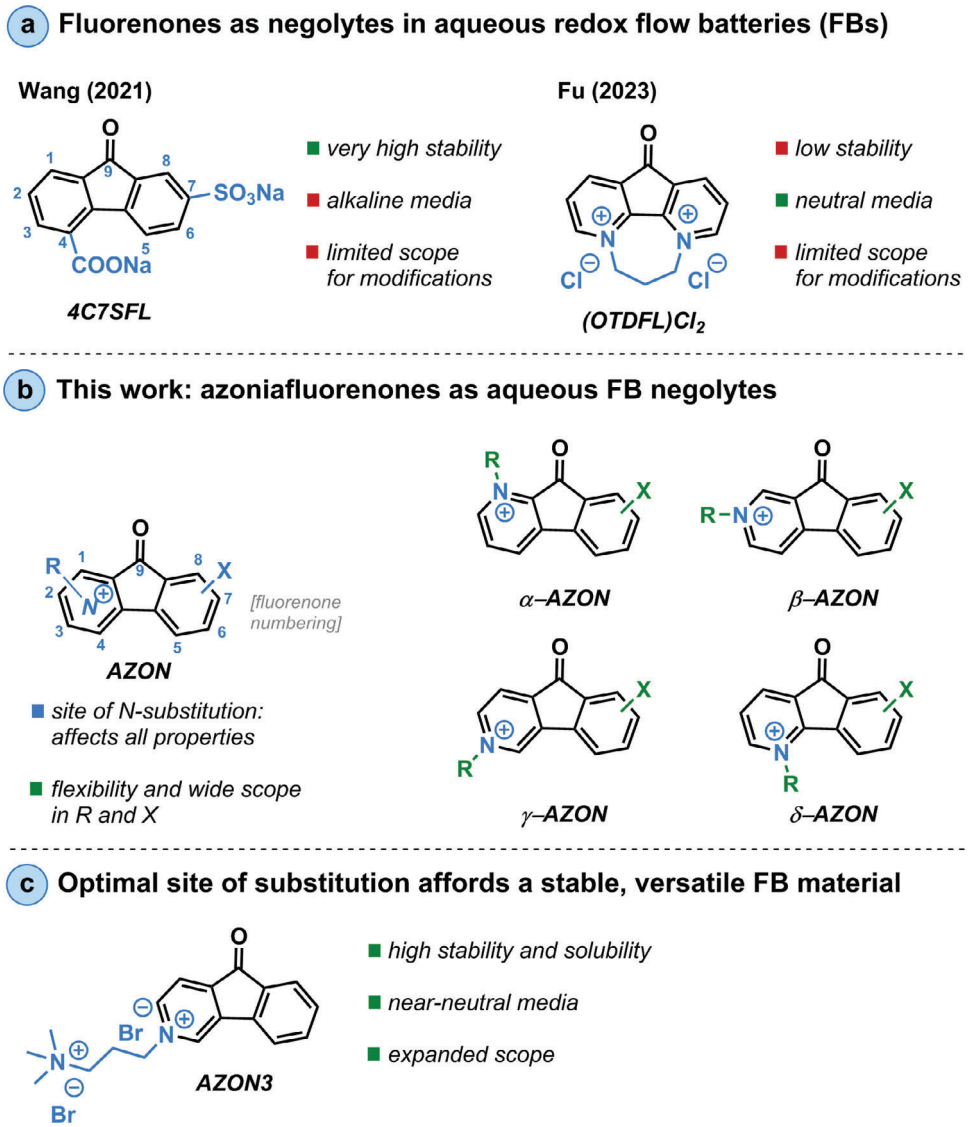

Figure 1. a) Fluorenones as potential two-electron negolytes in FBs: 4C7SFL and (OTDFL)Cl_2 for AOFBs. b) Overview of the potential of azoniafluorenone-based negolytes in AOFB (fluorenone numbering was used for clarity). c) The best results were obtained with **AZON3** (see text).

pH conditions, with 67.8% capacity retention over 250 cycles at 0.25 M of the negolyte. The high redox potentials of (OTDFL)Cl_2, −0.04 and −0.29 V versus Ag/AgCl, and stability issues, as well as the need to use alkaline media for 4C7SFL, are the main drawbacks of these fluorenone FB negolytes. Additionally, charging and discharging of 4C7SFL involves more complex disproportionation/comproportionation cycle, leading to decreased performance when operating at higher current densities at room temperature.[20]

Herein, we present the azoniafluorenone core, a new class of FB negolytes, to address these limitations as two-electron storage systems in near-neutral pH AOFBs (Figure 1b). The azoniafluorenones incorporate a quaternized pyridinium ring fused to an indanone ring system. The purpose of the pyridinium is to enhance solubility and to adjust the redox potential (Figure 1b). We hypothesized that the position of the nitrogen in the heterocyclic system should have a significant influence on the chemical and electrochemical properties, including solubility, stability, redox potential, and reversibility. In this study, we show that the 3-substituted **AZON3** demonstrates excellent solubility in aqueous media at neutral pH (up to 1.64 M in 1 M KCl) with two reversible electron-transfer processes in 1 M KCl at −0.31 and −0.58 V versus the Ag/AgCl reference electrode (−0.10 and −0.37 V versus Standard hydrogen electrode (SHE)). In addition, **AZON3** exhibited remarkable stability when evaluated in a flow battery as a negolyte even at a concentration of 1 M in 3 M KCl, paired with stable well-known posolyte **BTMAP-Fc**.[22] It achieved a coulombic efficiency above 99.94% and demonstrated capacity retentions of 99.95% and 99.91% per cycle (99.35% and 99.21% per day) when cycling with 1 and 2 electrons, respectively (Figure 1c). The battery exhibits an average cell voltage of 0.63 V due to the low potential of the BTMAP-Fc and a volumetric capacity of 46.4 Ah L^{-1} (87% of capacity utilization). The synthetic pathway to azoniafluorenones is highly modular and enables the synthesis of a wide

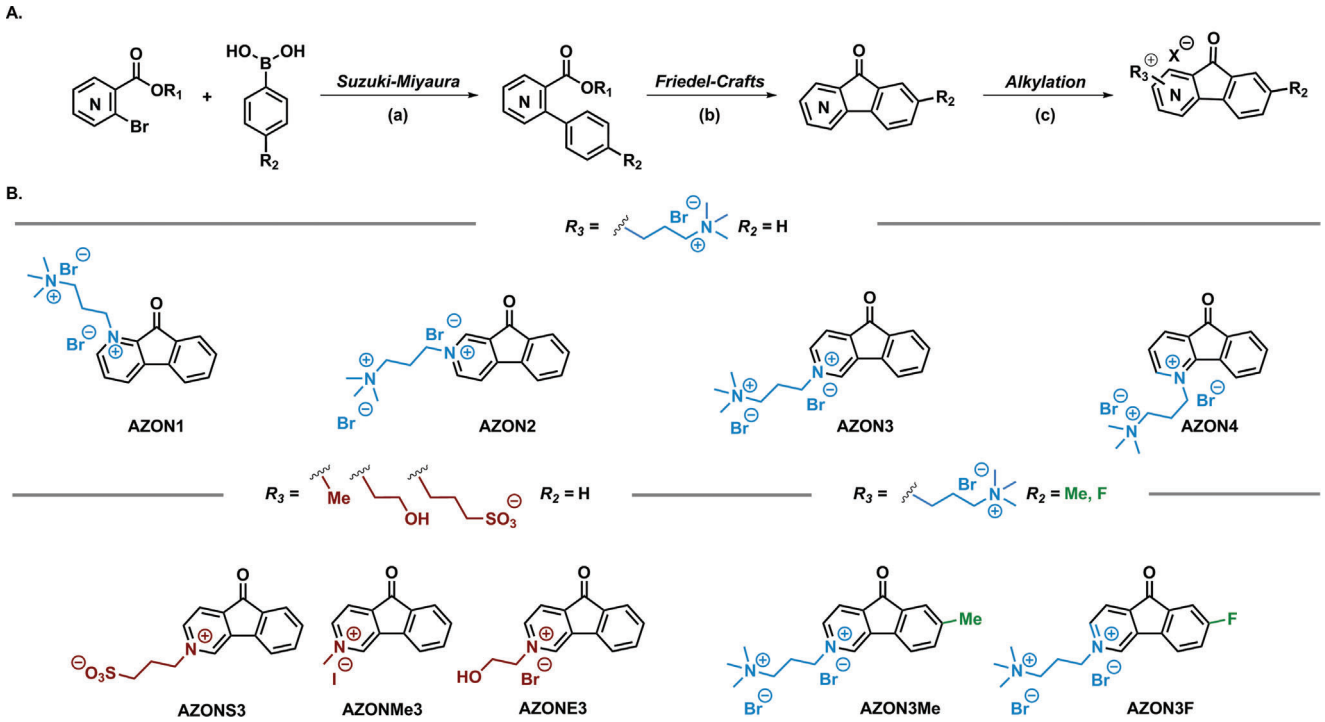

Scheme 1. A) General method for the synthesis of azoniafluorenone-based ammonium salts (see the Supporting Information); (a) $Pd(PPh_3)_4$ and K_2CO_3 in Toluene/H_2O at reflux overnight or $Pd(OAc)_2$, PPh_3 and K_2CO_3 in dimethoxyethane/H_2O at reflux overnight; (b) Polyphosphoric acid at 210 °C for 5 h; (c) For AZONMe3: MeI in DMF at 90 °C overnight (For other examples see the Supporting Information). B) Scope of the synthesized azoniafluorenone named AZON.

range of analogs similar to those explored within the viologen and anthraquinone family.[23,24]

2. Design of the New Family

A general method was designed to access azoniafluorenones (AZONs, **Scheme 1A**). The synthesis was initiated from the commercially available bromopyridine carboxylic acids, which were converted into the corresponding Me esters (see the Supporting Information). The esters were then subjected to Suzuki–Miyaura-coupling to afford the cyclization precursors. The corresponding carboxylic acids gave lower yields in the coupling step, presumably as a result of catalyst deactivation.

The *N*-substituted fluorenones were obtained by an intramolecular Friedel–Crafts reaction using polyphosphoric acid at 210 °C or thionyl chloride and $AlCl_3$ (see the Supporting Information). This reaction was typically carried out after saponification of the corresponding acid. However, with 7-Me or 7-F-substituents (fluorenone numbering), the cyclization could be carried out directly with the Me ester (see the Supporting Information). Next, several electrophiles were used in an alkylation reaction to produce the azoniafluorenones (Scheme 1A). As an example, **AZON3** was synthesized with an overall yield of 54% over five steps, requiring only a single purification using silica gel (see the Supporting Information), and the synthesis could be readily scaled up to a gram scale (see the Supporting Information). The choice of the *N*-substituents ranged from cationic, neutral, and anionic to examine their effects on solubility, reversibility, and stability.[25,26]

The synthetic route is versatile and scalable. By utilizing different boronic acids that are inexpensive and commercially available materials, it is possible to access a diverse range of AZONs derivatives, thereby opening opportunities to explore a wide spectrum of FB materials.

3. Electrochemical Investigations

Our investigation started by examining a group of four azoniafluorenone derivatives **AZON1**, **AZON2**, **AZON3**, and **AZON4**, differing in the site of the *N*-substitution. Initially, we decided to retain the quaternary ammonium in the side chain to enhance compound solubility and prevent unwanted reactions such as dimerization through coulombic repulsion (Scheme 1B).

We initially investigated the electrochemical behavior of these synthesized compounds using cyclic voltammetry (CV) in different electrolytes, including 1 M potassium chloride (KCl) and 0.1 M sodium hydroxide (NaOH) (see the Supporting Information for details). Surprisingly, **AZON2** and **AZON4** exhibited irreversible reduction peaks, suggesting instability of the reduced species. On the other hand, **AZON1** and **AZON3** demonstrated two highly reversible redox processes at low potentials in neutral media (1 M KCl, see the Supporting Information). In basic media (0.1 M NaOH), **AZON1** did not show any reduction peaks, while **AZON3** displayed two reversible peaks (see the Supporting Information). For **AZON3** in 1 M KCl, the redox potentials correspond to −0.31 and −0.58 V versus Ag/AgCl reference electrode. In the basic medium (0.1 M NaOH), the potential of the second reduction event remained constant, whereas the first event shifted

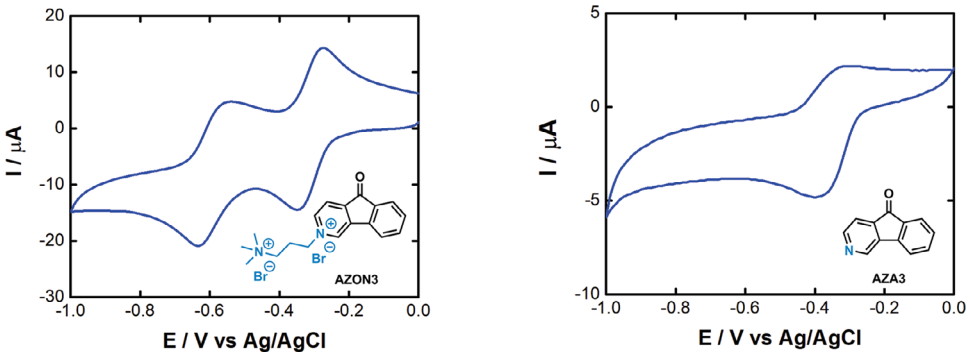

Figure 2. Cyclic voltammograms of 1 mM of **AZON3** and **AZA3** at 100 mV s^{-1} scan rate in 1 M KCl.

toward more negative values, suggesting a proton-coupled electron transfer (PCET) process. Overall, the redox potentials of **AZON3** are significantly lower compared to (OTDFL)Cl_2, leading to higher cell voltage and power density when applied in a flow battery.

A comparison of azafluorenone **AZA3** (**Figure 2**) and **AZON3** revealed that **AZA3** exhibited a poor reversible redox process in CV and very low solubility (< 5 mM) in 1 M KCl. This finding is consistent with previous results on (OTDFL)Cl_2[21] and confirms that the presence of the pyridinium moiety effectively improves both reversibility and solubility.

To further examine the stability of **AZON1** and **AZON3**, we conducted experiments in lab-scale flow batteries. The initial stability tests involved galvanostatic cycling using a 5 mM concentration of the redox material dissolved in 1 M KCl at pH 7 using an excess amount of BTMAP-Fc as the posolyte so the negolyte becomes the capacity-limiting side. The cell was assembled using a Selemion DSVN anionic exchange membrane and we performed all the tests inside a N_2-filled glovebox. Further information about the flow-cell tests is provided in the Supporting Information. In these conditions, when cycling the first electron, **AZON1** exhibited a capacity decay of 0.138% per cycle (5.70% per day) after 68 cycles; at higher pH, an increased capacity decay of 0.522% per cycle was observed, indicating lower stability under alkaline conditions. The proximity of the pyridinium group to the ketone moiety is hypothesized to contribute to this instability, as the electron-withdrawing effect of the pyridinium group can destabilize the reduced species, leading to degradation (see the mechanism study below). We also conducted a similar study on **AZON3**, using a concentration of 5 mM in 1 M KCl at pH 7. In this case, for one-electron cycling, the battery presented an initial capacity decay presumably due to oxygen content and then it remained stable for 75 cycles without any observed decay. After that, the cut-off voltage was increased to achieve the second electron process. The cycling under these conditions presented a decay of 0.179% per cycle, indicating a lower stability of the two-electron reduced species. Additionally, we investigated the stability of **AZON3** in a battery using 0.1 M NaOH as a supporting electrolyte, but the reduced form of the compound was inherently unstable under basic conditions. Consequently, we continued our research using a neutral-pH electrolyte to mitigate any potential stability issues associated with higher alkalinity. This study demonstrated that the position of the nitrogen on the fluorenone ring plays a crucial role in the stability of this redox material, making **AZON3** a strong candidate for AOFBs, warranting further investigation. However, it remains uncertain whether the favorable results come from the quaternary ammonium substituent or the nature of the pyridinium moiety itself.

Additional experiments with *N*-substituted variants, such as methyl (**AZONMe3**), hydroxyethyl (**AZONE3**), and propane sulfonate (**AZONS3**) (Scheme 1B), were carried out to solve this uncertainty. Under CV measurements, all three compounds displayed good reversibility in both 1 M KCl and 0.1 M NaOH (see the Supporting Information for CVs). However, **AZONMe3** and especially **AZONS3** showed poor solubility in aqueous media and as such, **AZONS3** was omitted from further investigation. In the case of **AZONMe3**, we assembled a battery at low concentration (1 mM) in 1 M KCl that remains stable when cycling one electron with no capacity decay over 70 cycles, however, just a small percent of the total capacity was cycled (20%). We attribute the low accessible capacity to the poor solubility of **AZONMe3**. This result suggests that polar groups alone should enhance the solubility and accessible capacity of **AZONMe3** and make it a promising candidate for AOFBs. Indeed, **AZONE3**, with an additional OH group in the molecule, demonstrated excellent solubility and it was tested at a concentration of 5 mM in lab-scale AOFBs in 1 M KCl, however, it showed a high capacity decay (0.518% per cycle) for one-electron cycling. The higher rate of decay of **AZONE3** compared to **AZON3** could be explained by the presence of the OH group, which can act as a nucleophile and attack the exocyclic *N*-substituted carbon (intra or intermolecularly) to give **AZA3** that cannot be oxidized back in the conditions studied. A similar side reaction has been reported previously for a related viologen derivative.[27]

Based on this evaluation, **AZON3** remained the most promising candidate. To gain further insight, the effect of electron-donating or withdrawing substituents in the second ring (Figure 1B) was investigated.[28] **AZON3Me** incorporates a methyl-donor group on position 7 of the fluorenone ring and **AZON3F** bears an electron-withdrawing fluorine substituent in the same position.

CV and battery tests revealed that **AZON3Me** exhibited similar redox behavior and stability that the parent **AZON3** compound, with no observable effect of the methyl donor substituent on redox potential or stability when tested in a flow-cell at low concentration (5 mM) in 1 M KCl (see the Supporting Information). Similarly, **AZON3F** demonstrated a similar redox profile to **AZON3**, albeit with a slight positive shift in standard potentials

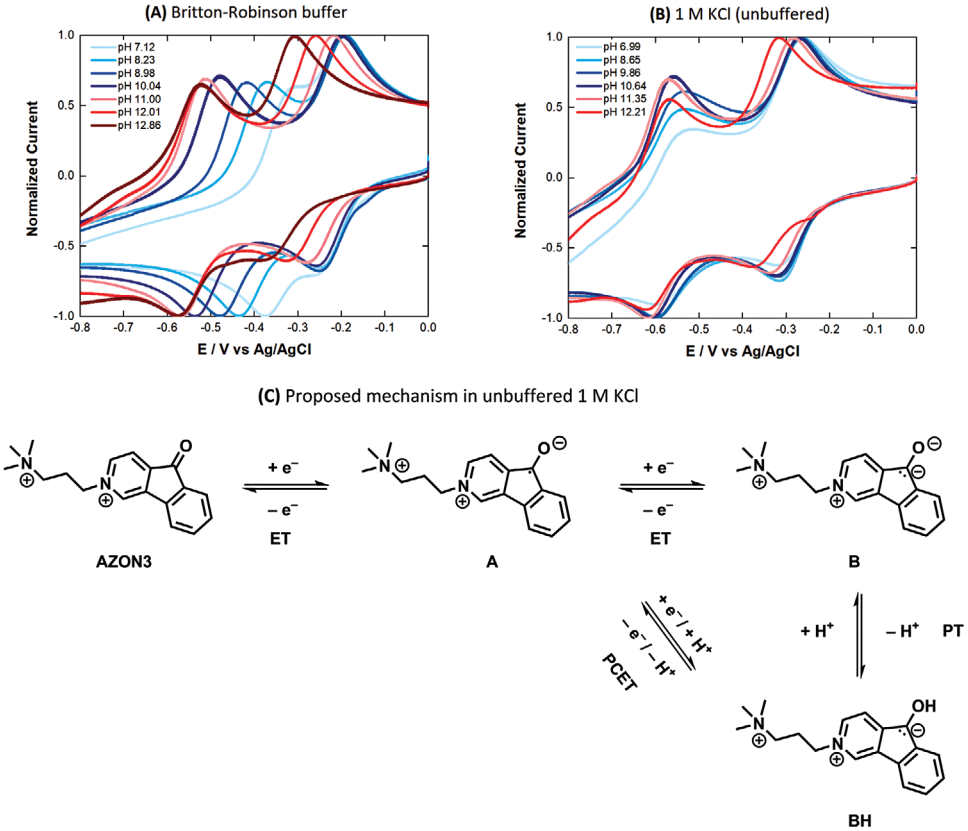

Scheme 2. Cyclic voltammograms of 1 mM of **AZON3** at 100 mV s^{-1} scan rate in A) 0.12 M Britton–Robinson buffer B) 1 M KCl at different pH values. Potentials reported against Ag/AgCl reference. C) Proposed mechanism in unbuffered 1 M KCl (counter anion omitted).

of 40 and 15 mV on the first and second redox process, respectively, without impacting stability when tested in a battery at low concentrations (5 mM) in 1 M KCl (see the Supporting Information). Although these studies did not indicate any improvements, these substituents nevertheless present suitable handles for further molecular diversification for future studies.

4. Mechanistic Discussion

We studied the mechanism of the redox process of **AZON3** by studying the relation between redox potential and pH. First, we used Britton–Robinson buffer electrolyte (0.12 M) and performed CVs at different pHs by adjusting with diluted KOH (**Scheme 2A**). The results show that, from pH 7 to 10, the potential of the first redox event remains constant while the second one shifts to more negative values with a slope of 57 mV per unit of pH, indicating a reaction involving one electron and one proton in the PCET reaction. Above pH 11, it presents the opposite behavior: the potential of the second electron remains constant while the first one becomes more negative (50 mV per unit of pH), also suggesting a PCET mechanism (see the Pourbaix diagram in the Supporting Information). Furthermore, we observed that the yellow color of **AZON3** sample immediately vanished as the pH was increased above 11, changing slowly to red after a few minutes. The red color faded upon exposure to the air. We hypothesize that **AZON3** is deprotonated at the *N*-CH_2 group in basic pH,[29] leading to undesired side reactions and species with a radical character that react with oxygen.[29] A more detailed study of these events was not conducted as our focus was on a negolyte that performs at near-neutral pH. Finally, we conclude that at neutral pH in a buffered solution, the reduction mechanism of **AZON3** consists of ET followed by PCET, which is in full agreement with the results obtained previously for $(OFTDL)Cl_2$.[21]

Next, the pH dependence of the redox process of **AZON3** was studied using an unbuffered KCl electrolyte (Scheme 2B). For the first electron, the potential remains constant until pH 11 where the potential starts shifting to a more negative value (31 mV per unit of pH), a similar behavior as in buffered electrolyte. However, the potential of the second redox event remains constant at a value of −0.58 V in the studied pH range. That value is similar to the potential of the second wave when working in the Britton–Robinson buffer solution at pH above 10, which suggests that in an unbuffered solution, the pH near the electrode surface increases as a result of the PCET that consumes protons. This effect has been reported and explained for quinones by Smith et al.[30] demonstrating that, in an unbuffered aqueous electrolyte, quinones are double reduced through two sequential 1 e^- transfers (double ET process), instead of the PCET event proposed for buffered electrolytes. In this study, we hypothesized that with **AZON3** in an unbuffered KCl electrolyte, the reduction proceeds via an ET which generates first the radical **A**, followed by either PCET or ET, depending on the local pH, forming the protonated reduced species **BH** or reduced species **B** with a pK_a between 10.5

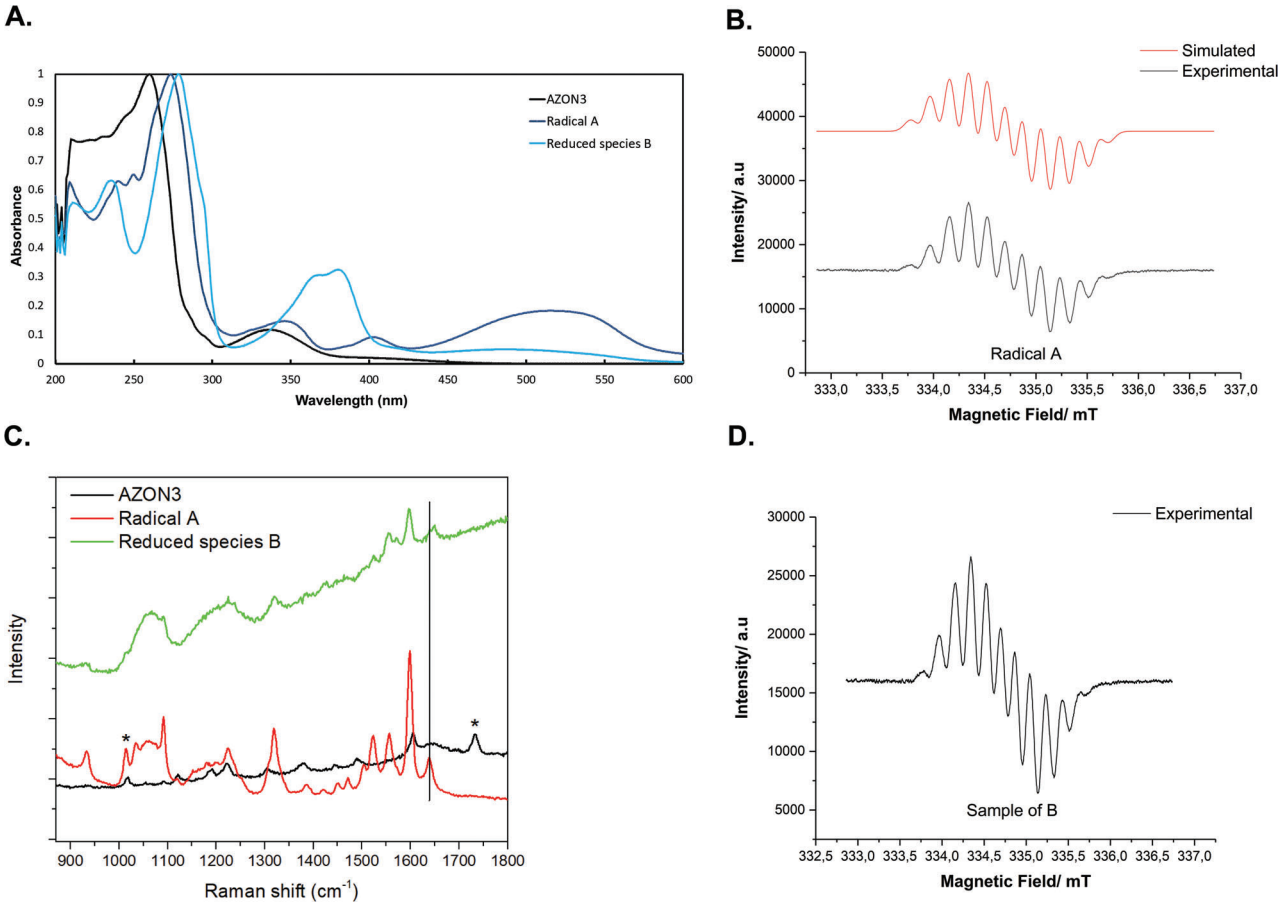

Figure 3. Characterization of radical **A** (one-electron-reduced species derived from **AZON3**) and reduced species **B** (two-electron-reduced species derived from **AZON3**). A. UV–vis spectra. B. EPR spectra of radical **A**, simulated and experimental results. C. Raman spectra of **AZON3**, **A** and **B**. D. EPR spectrum of a sample of **B**.

and 11 (Scheme 2C). The Pourbaix diagram of **AZON3** is presented in the Supporting Information. Once the pH reaches the pKa value of B, the second reduction continues as ET at a constant pH. At low **AZON3** concentration (1 mM), the second reduction proceeds via either ET or PCET, but as the concentration of **AZON3** increases, the pH reaches the pKa value immediately so we can assume that most of the mechanism corresponds to ET. This conclusion is also corroborated by the study of 4C7SFL in alkaline media where a similar reduction was observed.[20]

To further confirm the structures of reduced intermediates **A** and **B**, we characterized them using UV–vis, EPR, NMR, and Raman spectroscopy. **A** and **B** were generated in a flow cell in an O_2-free environment using unbuffered 1 M KCl as a supporting electrolyte. The latter offers a 300 mV separation between the two redox processes, allowing to study both reduced species separately by setting the appropriate cut-off voltages. Once the cut-off voltage was reached, this was held for a fixed time to ensure conversion to the reduced species. While the charged capacity during the experiments was in agreement with the expected theoretical capacity (see the Supporting Information), we cannot exclude the possibility of traces of the partially reduced species. In the UV–vis spectra, the addition of the first electron to **AZON3** was identified by the appearance of a large band at 520 nm (**Figure 3**A), which can be attributed to the radical form of the reduced compound **A**.[31,32] The structure of **A** was further corroborated by EPR measurements. While **AZON3** was initially EPR silent, the introduction of the first electron resulted in the formation of a species exhibiting a strong EPR signal (Figure 3B), consistent with the ketyl radical anion **A** and fitted by spectral simulation (Figure 3B). The NMR spectrum of **A** was nearly invisible, as anticipated for a paramagnetic species (see the Supporting Information). In addition, Raman spectroscopy of **AZON3** reveals a C=O stretching at 1732 cm^{-1} (Figure 3C). The one-electron reduction of **AZON3** into its radical anion **A** is confirmed by Raman, as evidenced by the disappearance of the band at 1732 cm^{-1}, and the appearance of new bands in the range from 1500 to 1655 cm^{-1} due to C=C and CO vibrations. This shift is fully consistent with the reduction of the C=O group of **AZON3** and the decrease of stretching frequency due to the population of an antibonding π^* orbital by the added electron.[33] The band at 1524 cm^{-1} can be assigned to the CO vibration of the radical anion **A** after the first reduction (Figure 3C). The band at 1014 cm^{-1} which remains unchanged after reduction is due to the ring breathing mode of the aromatic ring. All these spectral measurements support the suggested structure of **A** as a ketyl radical anion.

After further electrochemical reduction of **A** to **B**, the UV–vis spectrum of **B** displayed two new bands at 368 and 382 nm, which confirms the further reduction of the zwitterionic species. Furthermore, the reduction of **AZON3** leads to a shift of the large band from 265 to 275 and 280 nm, after the first and second electron addition, respectively (Figure 3A). Surprisingly, the sample of **B** also exhibited a strong EPR signal identical to the radical **A** (Figure 3D) and displayed a very low signal intensity in NMR (see the Supporting Information). We cannot exclude the possibility that a small concentration of **A** is still present in the sample of **B**, and the EPR signal observed for the two samples is essentially identical. Additional evidence for the build-up of **A** was provided by monitoring the evolution of the UV–vis spectra of a sample of **B** over 20 days, which displayed increasing absorption at 520 nm (see the Supporting Information) characteristic of **A** (see above). However, the Raman spectra of **A** and **B** are different, showing a shift of the peak at 1638 to 1648 cm^{-1} (**A** vs **B**, see Figure 3C). Furthermore, **B** shows a clear rise in the baseline indicating fluorescence that is not present in **A**, consistent with the notion that the electronic structure of **B** is distinct from **A**. Additionally, for **A**, we also observed a resonance Raman effect when using the 532 nm laser, but this was not observed with **B**. For **A**, the laser excitation frequency 532 nm closely matches the electronic transition frequency of the sample (see Figure 3A). Finally, we assume that a sample of **B** is partially oxidized back to **A** upon exposure to oxygen (see the Supporting Information). Taken together, the evidence suggests that **B** is the two-electron reduced form of **AZON3**, distinct from **A**.

During battery cycling in unbuffered KCl, we expected the upward pH shift due to the initial protonation of the reduced species in the ET-PCET until the pH reaches the pK_a of compound **BH** (≈10.5–11). After reaching that pH, the reduction proceeds by the double ET mechanism described above, in analogy to the description of the reduction of quinones in buffered/unbuffered solutions.[30] The CV measurements performed in buffer solution (Scheme 2A) demonstrated that the second redox process can be described as ET at pH above 11, and since the reaction does not consume more protons at this point, the pH does not increase more than that value. Considering that the redox reaction is a reversible process, the pH of the unbuffered solution fluctuates during cycling, increasing to a value close to 11 during charging (consuming protons) and decreasing during discharging (releasing protons). Aziz et al.[10] reported this behavior in the battery by studying the pH change during cycling for a phosphonate-functionalized quinone. In that work, they immersed a pH probe in the negolyte reservoir, and they were able to measure the pH change during charge and discharge. Here, we verified the electrolyte pH change during battery cycling of **AZON3** (5 mM concentration) in unbuffered KCl by measuring the pH of the negolyte at different stages (see the Supporting Information). The initial pH of the negolyte was 8.11 and then it was measured after charging and discharging the first electron, obtaining 9.35 and 8.80, respectively. Considering that the mechanism of the first electron process corresponds to ET, so it does not consume protons, we can assume that the slight pH shift in this stage occurs because the second electron is partially accessed. After that, the battery was cycled using two electrons, and the pH was measured after charge and discharge, resulting in 10.91 and 8.91, respectively. These measurements confirm the pH fluctuation during battery operation demonstrating that the pH does not increase above 11.

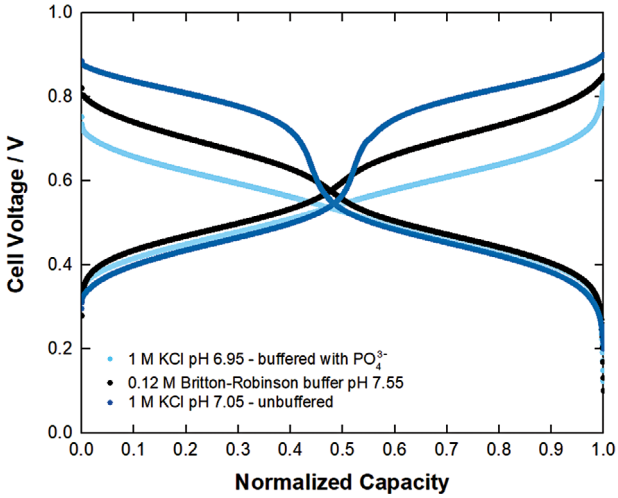

Figure 4. Cycling figures of 5 mM AZON3 flow batteries in different buffered and unbuffered electrolytes.

Furthermore, the proposed double ET mechanism occurring in unbuffered KCl is exhibited by the voltage separation between the plateaus of the first and second electrons (**Figure 4**). As expected from the CV measurements, at buffered neutral-pH conditions the cell voltages during the first and second electron processes are similar, while in unbuffered KCl they are separated by ≈300 mV. In order to check the stability in buffered electrolytes, we also performed the cycling tests at these conditions (see the Supporting Information), resulting in lower stability compared with unbuffered KCl. Furthermore, the unbuffered electrolyte also offers lower negolyte potential that allows the developing of higher cell voltage and power density (Figure 4). We then continued the studies at high concentrations of **AZON3** using unbuffered KCl electrolytes.

Finally, to clarify why **AZON1** and **AZON3** show reversible behavior in CVs while **AZON2** and **AZON4** do not, we note that with **AZON2** and **AZON4**, the reduced species were not stable. A simple rationalization involves the possibility of delocalization of the charge in **AZON3** as the ketyl anion and the pyridinium cation is in a consonant relationship (**Figure 5**). In contrast, in **AZON2**, these functionalities are in a dissonant relationship as the nitrogen atom is in the incorrect position. We suggest that the two-electron reduction of **AZON3** gives rise to a stable zwitterion that can be reoxidized in the battery, whereas the two-electron reduction of **AZON2** (C) affords an unstable species, that cannot be oxidized back or lead to degradation.

5. Further Battery Experiments with AZON3

Finally, we investigated the stability of the new azoniafluorenone core in flow batteries at high concentrations. The set of experiments included the testing of **AZON3** in symmetric and full-cells paired with an excess amount of 1 M **BTMAP-Fc** electrolyte as posolyte. The battery conditions were the same as for the low-concentration tests, using unbuffered KCl at neutral pH as supporting electrolyte and anionic exchange membrane Selemion

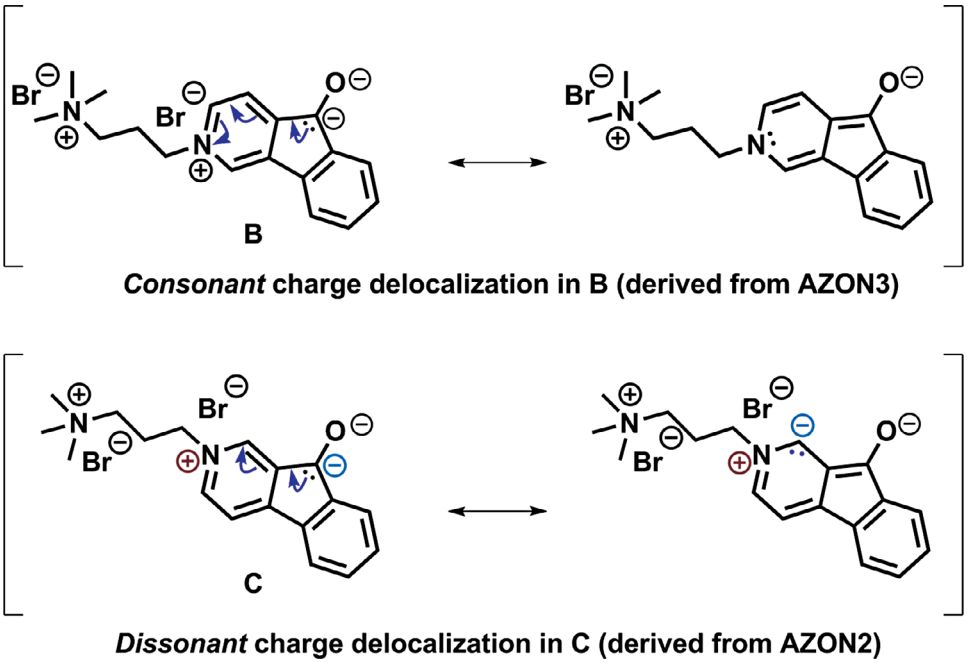

Figure 5. Delocalization structures of the reduced species of AZON2 and AZON3.

DSVN. All the tests were performed in a N_2-filled glove box at room temperature (30 °C). The battery tests consisted of galvanostatic cycling with potential holds at the end of each charge and discharge until the current density gets to a low value (2–10 mA cm^{-2}). Furthermore, we set different voltage cut-offs to evaluate the stability of the first and second electrons separately. Detailed depiction of the cell tests is included in the Supporting Information.

The first test consisted of a symmetric cell with 1 M concentration of **AZON3** and one-electron-cycling in 3 M KCl. The battery was run for almost 150 cycles until a tubing connector became blocked with solid material. Furthermore, during the test, we noticed a small electrolyte evaporation, so the corresponding amount of water was added to keep the 1 M concentration. When water was added, the battery recovered a high fraction of the capacity lost until that cycle, indicating that the reduced form of **AZON3** appears to be within the limits of its solubility in the supporting electrolyte. Excluding the capacity loss due to the solubility issue, the battery exhibited stable operation, with only 0.044% irreversible capacity fade rate per cycle (0.56% per day), with high capacity utilization (83%) and coulombic efficiency (99.97%). The same battery electrolytes were diluted to 0.56 M concentration in 2 M KCl to continue the testing in a second symmetric battery. In this case, a stable operation with a capacity fade rate of 0.029% per cycle (1.05% per day) over 200 cycles was observed while the coulombic efficiency remained high and unchanged. The slightly higher capacity fade rate observed in the second experiment can be attributed to possible degradation products remaining in the electrolytes and the cells from the previous experiment.

Then, we performed the two-electron cycling in a symmetric cell. For this, the electrolyte used in the previous experiment was charged to 100% SOC and diluted to obtain 0.46 M singly reduced species of AZON3 in 1.5 M KCl. This electrolyte was divided into both sides and two-electron cycling was performed with the same operation parameters but using a higher cut-off voltage in order to achieve the second electron. This battery presented high stability with a low capacity fade rate of 0.010% per cycle (0.27% per day) and a coulombic efficiency of 99.98% for more than 1000 cycles (**Figure 6**). During this long cycling, it was also necessary to add water to compensate for the amount lost because of evaporation, again evidencing a capacity recovery after each addition. We associate the reported irreversible capacity fade rates with chemical decomposition because the crossover effect is eliminated

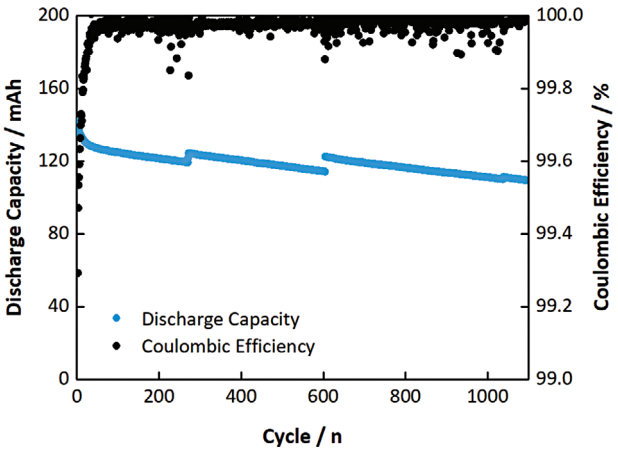

Figure 6. AZON3 symmetric cell 0.46 M performance for two-electron cycling: capacity and coulombic efficiency evolution. Supporting electrolyte: 1.5 M KCl. Addition of water to compensate for the amount lost by evaporation in cycles 270 and 604.

during symmetric cell testing and the capacity lost due to precipitation was already considered.[34]

The last battery test consisted of a full cell of **AZON3** 1 M as the negolyte, paired with an excess amount of **BTMAP-Fc** 1 M on the positive side. The electrolyte was 3 M KCl (unbuffered) with a slightly higher pH of 7.75 while the rest of the operation conditions were the same as described for the symmetric cells mentioned above. The first test consisted of one-electron cycling over 40 cycles, obtaining a similar performance to the symmetric cell with a capacity fade rate of 0.044% per cycle (0.65% per day) and high coulombic efficiency (99.95%). Even though it was short cycling, the similar behavior suggests that there is no crossover of **AZON3** through the membrane that leads to an additional capacity lost in the full cell set-up. Having validated the high stability of the first redox process, we then increased the cut-off voltage to study the second electron. In those conditions, the battery exhibited a cell voltage of 0.63 V and a large volumetric capacity reaching 46.4 Ah L^{-1} with 87% capacity utilization. Furthermore, the cell still showed relatively high stability with a low capacity fade rate of 0.097% per cycle (0.79% per day) and high coulombic efficiency (99.94%) for over 170 cycles (**Figure 7**). After cycling, the battery was stopped to perform post-mortem analysis. From the cyclic voltammetry studies of the electrolytes after cycling, we did not notice any crossover of the active species through the membrane confirming the similar results obtained with the 1 M symmetric cell.

During cycling at 60 mA cm^{-2} with a non-optimized lab-scale cell, the battery exhibited an energy density of 23.8 Wh L^{-1} with round trip efficiency of 65%, which is comparable with other organic materials reported,[35] e.g., the BTMAP-Fc/BTMAP-Vi cell reported by Aziz[22] with an efficiency of 60% when operated at that current density. Further tests to study power and energy densities were not conducted in this work, as these parameters are also influenced by cell architecture and the selected posolyte material. In this case, with the aim of demonstrating the azoniafluorenone family as a stable promising negolyte for AOFBs, BTMAP-Fc was selected because of its high stability and solubility,[22] however it exhibits a low redox potential of 0.39 V versus SHE, and as such it will not produce a highly competitive cell voltage.

Next, we studied the electrochemical kinetics of **AZON3**. We estimated the rate constants k^0 of both electron transfer reactions using the method of Nicholson.[36] First, the diffusion coefficient (D) of the oxidized form was calculated using Randles–Ševčík equation, obtaining a value of 3.98×10^{-6} cm^2 s^{-1}. Then, the estimated kinetic rate constants ($k^0{}_1$ and $k^0{}_2$) of the first and second electron transfer reactions were 9.52×10^{-2} and 6.07×10^{-2} cm s^{-1}, respectively, corresponding to fast kinetics rates when comparing with the rest of organic negolytes reported for AOFBs.[37]

This study demonstrated that the high solubility and two-electron storage of azoniafluorenone compounds lead to impressive specific capacities with relatively high capacity retention. The 1 M battery already exhibited a volumetric capacity of 46.4 Ah L^{-1}, which is one of the highest values reported for pH-neutral AOFBs[35,37] (see the Supporting Information), even higher than VFB. We next performed solubility tests using UV–vis and confirmed that **AZON3** can be dissolved up to 1.64 M in 1 M KCl, which would lead to a theoretical specific capacity of 88 Ah L^{-1}, an outstanding value within the AOFB negolytes.

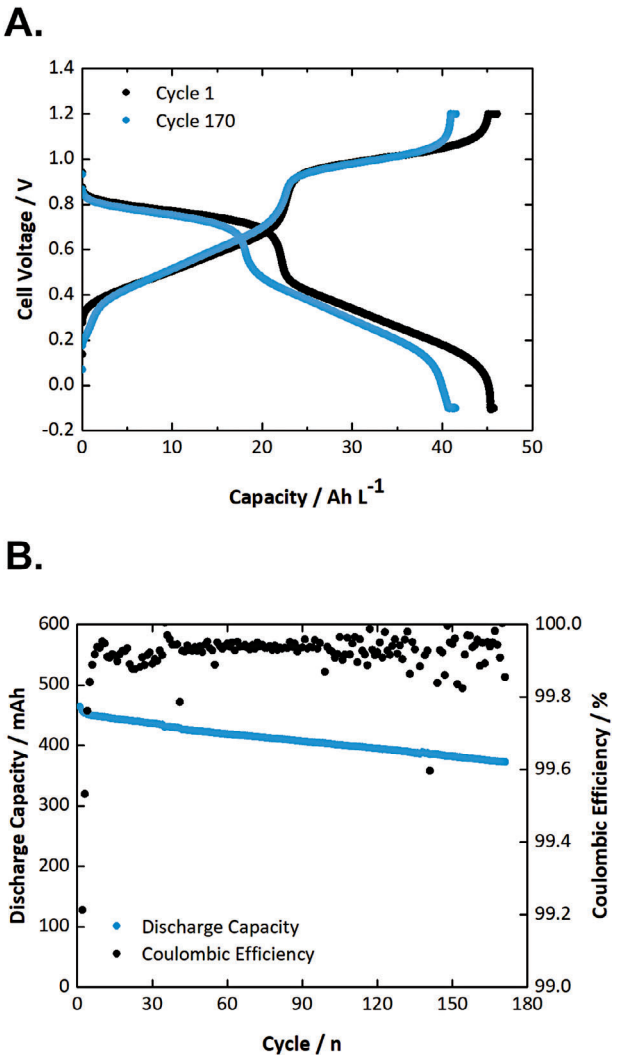

Figure 7. AZON3 full cell 1 M performance in a two-electron cycling experiment. Supporting electrolyte: 3 M KCl. Posolyte: 1 M BTMAP-Fc (excess). A) Charge and discharge profiles of cycles 1 and 170. B) Capacity and coulombic efficiency evolution.

These results have shown that, at near-neutral pH, azoniafluorenone shows very promising behavior as a negolyte for AOFBs. Considerable opportunities remain for further optimization and development of azoniafluorenone-based system to fully characterize its capabilities as a negative electrolyte.

6. Conclusion

In summary, this study introduces a new family of compounds based on the azoniafluorenone structure that shows promise as redox-active molecules for storing two electrons in AOFBs at near-neutral pH. Among the tested compounds, **AZON3** stands out for its high solubility of 1.64 M in 1 M KCl, which coupled with its capability of storing two electrons, leads to high-energy storage density (already demonstrated 46.4 Ah L^{-1}). Furthermore, it presents two highly reversible redox processes at relatively low potentials of −0.31 and −0.58 V versus Ag/AgCl/3 M KCl

reference (−0.10 and −0.37 V vs SHE). These processes involve ET followed by PCET or ET depending on the local pH of the solution. Finally, the flow cell tests confirmed the high stability of **AZON3** with a capacity fade rate of 0.010% per cycle in a symmetric cell at 0.46 M, and 0.097% capacity fade in a full cell at 1 M (87% of capacity utilization). Additionally, the developed synthetic pathway allows additional substitution in several positions (position 1,2,4,5,6,8 in the fluorenone skeleton), offering exciting opportunities for future exploration and optimization. These findings position **AZON3** as a leading compound in the field of AOFBs with the potential for efficient and reliable energy storage systems.

Supporting Information

Supporting Information is available from the Wiley Online Library or from the author.

Acknowledgements

M.A. and G.G. contributed equally to this work. This project has received funding from the European Union – NextGenerationEU instrument and is funded by Research Council Finland under grant numbers 348326 (P.P.) and 348328 (P.M.P.). Support from the European Union's Horizon2020 Research and Innovation programme under grant agreement No 875565 (Project CompBat) is also acknowledged. GG gratefully acknowledges the financial support from the University of Turku Graduate School. P.P. gratefully acknowledges the Academy Research Fellow funding (grant no. 315739, 343791, 320071, and 343794) from Research Council Finland, and European Research Council through a Starting grant (agreement no. 950038). Materials Analysis and Research Infrastructure (MARI) of the Univeristy of Turku was utilized in this work.

Conflict of Interest

The authors declare no conflict of interest.

Data Availability Statement

The data that support the findings of this study are available in the supplementary material of this article.

Keywords

azoniafluorenones, electrochemistry, energy storage, flow batteries, pyridinium ions

Received: April 10, 2024
Revised: June 13, 2024
Published online:

[1] J. Rugolo, M. J. Aziz, *Energy Environ. Sci.* **2012**, *5*, 7151.
[2] P. Alotto, M. Guarnieri, F. Moro, *Renew. Sustain. Energy Rev.* **2014**, *29*, 325.
[3] C. Roth, J. Noack, M. Skyllas-Kazacos, *Flow Batteries: From Fundamentals to Applications*, John Wiley & Sons, Hoboken NJ **2022**.
[4] M. L. Perry, K. E. Rodby, F. R. Brushett, *ACS Energy Lett.* **2022**, *7*, 659.
[5] L. Zhang, R. Feng, W. Wang, G. Yu, *Nat. Rev. Chem.* **2022**, *6*, 524.
[6] K. Lourenssen, J. Williams, F. Ahmadpour, R. Clemmer, S. Tasnim, *J. Energy Storage.* **2019**, *25*, 100844.
[7] G. Yang, Y. Zhu, Z. Hao, Y. Lu, Q. Zhao, K. Zhang, J. Chen, *Adv. Mater.* **2023**, *35*, 2301898.
[8] M. Pan, M. Shao, Z. Jin, *SmartMat.* **2023**, *4*, e1198.
[9] K. Peng, G. Tang, C. Zhang, X. Yang, P. Zuo, Z. Xiang, Z. Yao, Z. Yang, T. Xu, *J. Energy Chem.* **2024**, *96*, 89.
[10] Y. Ji, M.-A. Goulet, D. A. Pollack, D. G. Kwabi, S. Jin, D. De Porcellinis, E. F. Kerr, R. G. Gordon, M. J. Aziz, *Adv. Energy Mater.* **2019**, *9*, 1900039.
[11] J. Asenjo-Pascual, C. Wiberg, M. Shahsavan, I. Salmeron-Sanchez, P. Mauleon, J. R. Aviles Moreno, P. Ocon, P. Peljo, *ACS Appl. Mater. Interfaces.* **2023**, *15*, 36242.
[12] G. Tang, Z. Yang, T. Xu, *Cell Rep. Phys. Sci.* **2022**, *3*, 101195.
[13] C. Wang, X. Li, B. Yu, Y. Wang, Z. Yang, H. Wang, H. Lin, J. Ma, G. Li, Z. Jin, *ACS Energy Lett.* **2020**, *5*, 411.
[14] A. Hollas, X. Wei, V. Murugesan, Z. Nie, B. Li, D. Reed, J. Liu, V. Sprenkle, W. Wang, *Nat. Energy.* **2018**, *3*, 508.
[15] C. DeBruler, B. Hu, J. Moss, X. Liu, J. Luo, Y. Sun, T. L. Liu, *Chem.* **2017**, *3*, 961.
[16] X. Liu, X. Zhang, G. Li, S. Zhang, B. Zhang, W. Ma, Z. Wang, Y. Zhang, G. He, *J. Mater. Chem. A.* **2022**, *10*, 9830.
[17] M. Wu, Y. Jing, A. A. Wong, E. M. Fell, S. Jin, Z. Tang, R. G. Gordon, M. J. Aziz, *Chem.* **2020**, *6*, 1432.
[18] C. Wang, Z. Yang, B. Yu, H. Wang, K. Zhang, G. Li, Z. Tie, Z. Jin, *J. Power Sources.* **2022**, *524*, 231001.
[19] J. Rodriguez, C. Niemet, L. D. Pozzo, *ECS Trans.* **2019**, *89*, 49.
[20] R. Feng, X. Zhang, V. Murugesan, A. Hollas, Y. Chen, Y. Shao, E. Walter, N. P. N. Wellala, L. Yan, K. M. Rosso, W. Wang, *Science.* **2021**, *372*, 836.
[21] W. Li, J. Li, X. Yuan, Z. Xiang, Z. Liang, Z. Fu, *J. Mater. Chem. A.* **2023**, *11*, 19308.
[22] E. S. Beh, D. De Porcellinis, R. L. Gracia, K. T. Xia, R. G. Gordon, M. J. Aziz, *ACS Energy Lett.* **2017**, *2*, 639.
[23] J.-M. Fontmorin, S. Guiheneuf, T. Godet-Bar, D. Floner, F. Geneste, *Curr. Opin. Colloid Interface Sci.* **2022**, *61*, 101624.
[24] Y. Cho, H. Kye, B.-G. Kim, J. E. Kwon, *J. Ind. Eng. Chem.* **2024**, *136*, 73.
[25] M. Hu, W. Wu, J. Luo, T. L. Liu, *Adv. Energy Mater.* **2022**, *12*, 2202085.
[26] Y. Liu, Y. Li, P. Zuo, Q. Chen, G. Tang, P. Sun, Z. Yang, T. Xu, *ChemSusChem.* **2020**, *13*, 2245.
[27] G. Tang, Y. Liu, Y. Li, K. Peng, P. Zuo, Z. Yang, T. Xu, *JACS Au.* **2022**, *2*, 1214.
[28] K. M. Pelzer, L. Cheng, L. A. Curtiss, *J. Phys. Chem. C.* **2017**, *121*, 237.
[29] F. Liao, W. Huang, B. Chen, Z. Ding, X. Li, H. Su, T. Wang, Y. Wang, H. Miao, X. Zhang, Y. Luo, J. Yang, G. Zhang, *Chem. Commun.* **2020**, *56*, 11287.
[30] M. Quan, D. Sanchez, M. F. Wasylkiw, D. K. Smith, *J. Am. Chem. Soc.* **2007**, *129*, 12847.
[31] E. Wagner-Czauderna, R. Lipka, M. K. Kalinowski, *Ber. Bunsenges. Phys. Chem.* **1997**, *101*, 668.
[32] A. Behrendt, S. M. Couchman, J. C. Jeffery, J. A. McCleverty, M. D. Ward, *J. Chem. Soc. Dalton Trans.* **1999**, *24*, 4349.
[33] A. Juneau, M. Frenette, *J. Phys. Chem. B.* **2021**, *125*, 1595.
[34] E. Fell, M. Aziz, *J. Electrochem. Soc.* **2023**, *170*, 100507.
[35] Z. Li, T. Jiang, M. Ali, C. Wu, W. Chen, *Energy Storage Mater.* **2022**, *50*, 105.
[36] R. S. Nicholson, *Anal. Chem.* **1965**, *37*, 1351.
[37] V. Singh, S. Kim, J. Kang, H. R. Byon, *Nano Res.* **2019**, *12*, 1988.